

# **Magnetic and electronic properties of magnetite across the high pressure anomaly**

D. P. Kozlenko<sup>1\*</sup>, L. S. Dubrovinsky<sup>2</sup>, S. E. Kichanov<sup>1</sup>, E. V. Lukin<sup>1</sup>, V. Cerantola<sup>3</sup>,  
A. I. Chumakov<sup>3</sup>, and B. N. Savenko<sup>1</sup>

<sup>1</sup> Frank Laboratory of Neutron Physics, Joint Institute for Nuclear Research, 141980 Dubna, Russia

<sup>2</sup> Bayerisches Geoinstitut, Universität Bayreuth, D-95440 Bayreuth, Germany

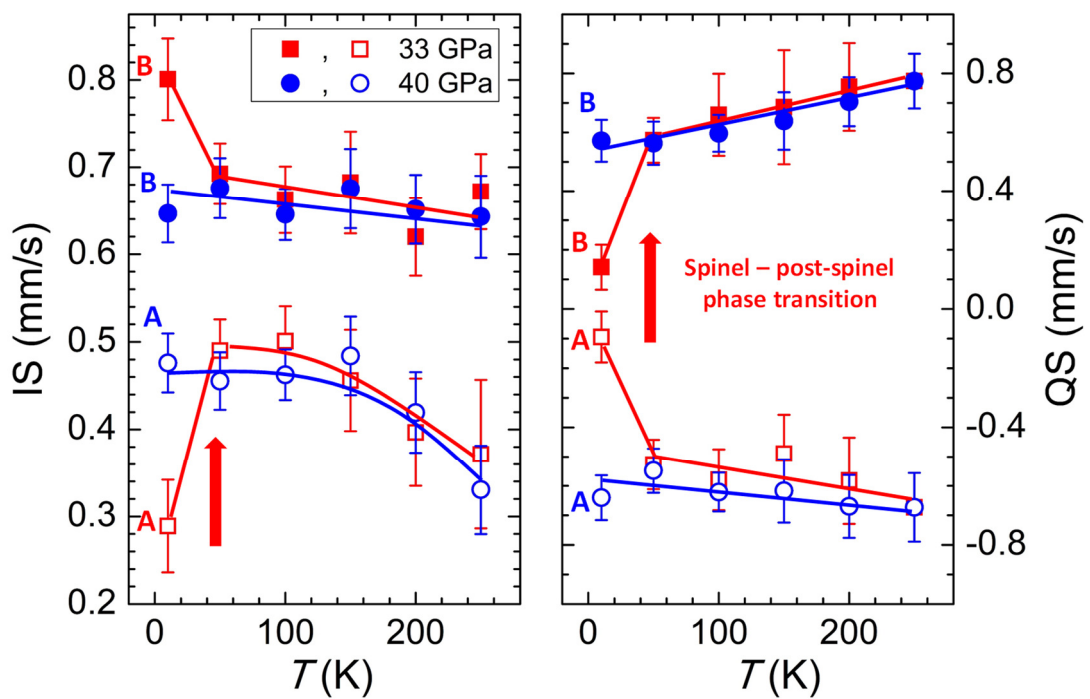
<sup>3</sup> European Synchrotron Radiation Facility, BP 220, F-38043 Grenoble, France

---

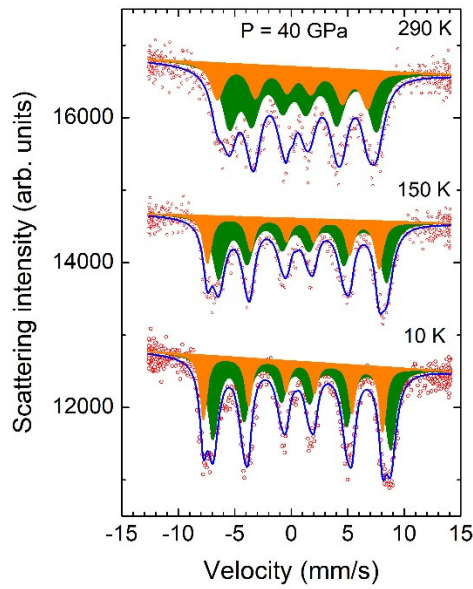
\* Corresponding author, e-mail denk@nf.jinr.ru

**Supplementary Table 1.** The hyperfine parameters of magnetite at selected pressures and temperatures.

$P, T$	$IS_A$ (mm/s)	$IS_B$ (mm/s)	$QS_A$ (mm/s)	$QS_B$ (mm/s)	$H_{hfA}$ (T)	$H_{hfB}$ (T)
8 GPa						
290 K	0.28(4)	0.71(3)	-0.03(7)	0.04(8)	48.4(2)	47.1(2)
250 K	0.30(2)	0.72(2)	-0.07(4)	0.05(3)	48.5(2)	47.4(1)
200 K	0.34(2)	0.72(2)	-0.01(2)	0.03(2)	49.1(2)	47.8(1)
150 K	0.41(4)	0.77(3)	-0.01(6)	-0.04(5)	49.5(4)	48.1(2)
100 K	0.41(4)	0.76(3)	0.004(5)	-0.02(4)	49.6(2)	48.4(2)
50 K	0.38(3)	0.82(5)	-0.03(7)	-0.04(7)	50.4(2)	50.3(2)
10 K	0.29(5)	0.38(3) ( $Fe^{3+}$ ) 1.03(4) ( $Fe^{2+}$ )	0.3(1)	-0.6(1) ( $Fe^{3+}$ ) -0.5(1) ( $Fe^{2+}$ )	50.6(1)	50.5(1) ( $Fe^{3+}$ ) 50.5(2) ( $Fe^{2+}$ )
21 GPa						
290 K	0.22(3)	0.63(2)	-0.04(5)	-0.01(4)	48.0(2)	47.2(2)
250 K	0.29(3)	0.65(2)	0.02(4)	0.01(4)	48.2(2)	47.4(2)
200 K	0.22(4)	0.70(3)	-0.08(8)	-0.04(6)	48.2(3)	47.9(2)
150 K	0.35(4)	0.74(3)	-0.01(6)	0.01(6)	48.5(2)	48.0(2)
100 K	0.41(3)	0.77(4)	0.00(5)	0.04(7)	49.0(2)	47.8(2)
50 K	0.43(3)	0.78(4)	-0.10(6)	0.10(7)	48.9(2)	47.8(2)
10 K	0.35(4)	0.79(4)	-0.01(7)	0.06(6)	48.9(2)	48.4(2)
33 GPa						
290 K spinel	0.26(8)	0.60(8)	-0.08(9)	-0.12(9)	47.8(6)	47.3(6)
post-spinel	0.34(7)	0.73(7)	-0.32(10)	0.66(10)	40.2(8)	38.5(8)
250 K	0.37(5)	0.68(5)	-0.52(10)	0.89(10)	40.8(3)	40.5(3)
200 K	0.40(5)	0.62(5)	-0.43(10)	0.78(10)	43.8(3)	43.1(3)
150 K	0.44(5)	0.67(5)	-0.47(9)	0.63(9)	46.5(3)	45.9(3)
100 K	0.50(5)	0.65(5)	-0.60(9)	0.63(9)	48.2(2)	47.5(2)
50 K	0.49(5)	0.69(5)	-0.52(7)	0.57(8)	49.2(2)	48.2(2)
10 K	0.29(5)	0.80(5)	-0.09(7)	0.14(7)	48.9(2)	48.6(2)
40 GPa						
290 K	0.39(5)	0.64(5)	-0.55(10)	0.77(1)	41.2(3)	40.3(3)
250 K	0.33(5)	0.64(5)	-0.66(10)	0.77(10)	42.9(3)	41.9(3)
200 K	0.42(4)	0.65(4)	-0.67(9)	0.71(9)	45.2(3)	44.2(3)
150 K	0.48(4)	0.67(4)	-0.62(9)	0.64(9)	47.1(3)	46.1(3)
100 K	0.46(3)	0.66(3)	-0.62(7)	0.59(7)	48.4(2)	47.8(2)
50 K	0.46(3)	0.67(3)	-0.55(7)	0.56(7)	49.0(2)	48.4(2)
10 K	0.48(3)	0.65(3)	-0.64(7)	0.57(7)	49.1(2)	48.7(2)



**Supplementary Figure 1.** Temperature behavior of the isomer shifts and quadrupole splittings of  $\text{Fe}_3\text{O}_4$  at  $P = 33$  and  $40$  GPa. The open and solid symbols correspond to (A) tetrahedral sites of iron in the spinel phase or bicapped trigonal prismatic sites in the post-spinel phase and (B) octahedral sites of iron in both phases. The spinel – post-spinel phase transition point is marked by arrow.



**Supplementary Figure 2.** The SMS spectra of  $\text{Fe}_3\text{O}_4$ , measured at  $P = 40 \text{ GPa}$  and selected temperatures. The experimental points, fitting curves and the sextet components, corresponding to the bicapped trigonal prismatic (orange color) and octahedral sites (olive color) in the post-spinel phase are presented.

### Supplementary Table 2

Structural parameters of the post-spinel phase of  $\text{Fe}_3\text{O}_4$  with the orthorhombic crystal structure of  $Bbmm$  symmetry at  $P = 33 \text{ GPa}$  and ambient temperature.

		$a (\text{\AA})$	$b (\text{\AA})$	$c (\text{\AA})$
Lattice parameters		9.246(5)	9.278(5)	2.763(3)
Coordinates				
Atom type	Position	$x$	$y$	$z$
Fe1	$4c$	0.377	0.25	0
Fe2	$8f$	0.131	0.077	0
O1	$4b$	0.5	0	0
O2	$4c$	0.033	0.25	0
O3	$8f$	0.215	0.616	0